ISSN 0735-1097/03/$30.00
doi:10.1016/S0735-1097(03)00581-3

# Ultrasound Tissue Characterization Detects Preclinical Myocardial Structural Changes in Children Affected by Duchenne Muscular Dystrophy

Vincenzo Giglio, MD,*† Vincenzo Pasceri, MD, PHD,‡ Loredana Messano, MD,*§ Fortunato Mangiola, MD,* Luciano Pasquini, MD,‖ Antonio Dello Russo, MD,*§ Antonello Damiani, MD,* Massimiliano Mirabella, MD, PHD,*¶ Giuliana Galluzzi, MD, PHD,*¶ Pietro Tonali, MD,¶# Enzo Ricci, MD*¶

*Rome and San Giovanni Rotondo, Italy*

**OBJECTIVES** Our goal was to identify early changes in myocardial physical properties in children with Duchenne muscular dystrophy (DMDch).

**BACKGROUND** Duchenne muscular dystrophy (DMD) is caused by the absence of dystrophin, which triggers complex molecular and biological events in skeletal and cardiac muscle tissues. Although about 30% of patients display overt signs of cardiomyopathy in the late stage of the disease, it is unknown whether changes in myocardial physical properties can be detected in the early (preclinical) stages of the disease.

**METHODS** We performed an ultrasonic tissue characterization (UTC) analysis of myocardium in DMDch with normal systolic myocardial function and no signs of cardiomyopathy. Both the cyclic variation of integrated backscatter (cvIBS) and the calibrated integrated backscatter (cIBS) were assessed in 8 myocardial regions of 20 DMDch, age 7 ± 2 years (range 4 to 10 years), and in 20 age-matched healthy controls.

**RESULTS** We found large differences in the UTC data between DMDch and controls; the mean value of cvIBS was 4.4 ± 1.5 dB versus 8.8 ± 0.8 dB, whereas the mean value of cIBS was 36.4 ± 7.1 dB versus 26.9 ± 2.0 dB ($p < 10^{-6}$ for both). In DMDch, all eight sampled segments showed cIBS mean values to be significantly higher and cvIBS mean values to be significantly lower than those in the controls. Finally, interindividual differences were greater in DMDch than in controls for both parameters.

**CONCLUSIONS** The myocardium in DMDch displays UTC features different from those in healthy controls. These results show that lack of dystrophin is commonly associated with changes in myocardial features well before the onset of changes of systolic function and overt cardiomyopathy. (J Am Coll Cardiol 2003;42:309–16) © 2003 by the American College of Cardiology Foundation

Duchenne muscular dystrophy (DMD) is an X-linked recessive disorder that affects approximately 1 of 3,500 male births and is caused by the absence of dystrophin, a 427-kd protein located on the inner sides of the skeletal and cardiac muscle cells. Dystrophin links the muscle cytoskeleton to the extracellular matrix by interacting with a large number of membrane proteins (1), and it might also play a role in the regulation or localization of signal transduction molecules (2). Absence of dystrophin generates progressive damage of skeletal muscle, causing a decrease in function that is clinically evident in childhood, although subtle histological changes may occur earlier (3,4).

See page 317

Absence of dystrophin triggers a dystrophic process also in the myocardium, accounting for the severe fibrosis found at endomyocardial biopsy (5) and postmortem (6) examination. Although characteristic electrocardiographic changes become evident in 80% to 90% of DMD children (DMDch) over 10 years of age (7), cardiomyopathic symptoms emerge in only about 30% of cases (8). However, it is not clear whether early changes in myocardial physical properties may be present even in asymptomatic DMDch who have normal electrocardiogram (ECG) and left ventricular systolic function. No previous study has shown any changes in myocardial features in these patients. Ultrasonic tissue characterization (UTC) can be used to obtain a noninvasive characterization of the physical properties of the myocardium. Mori et al. (9) recently described UTC abnormalities in a group of 25 relatively old DMD patients (17.6 ± 2.7 years), most of whom showed overt cardiomyopathy. In the present study, we used UTC to detect early changes in myocardial physical properties in asymptomatic DMDch with no other signs of cardiac involvement and with normal ECG and left ventricular systolic function.

From the *Center for Neuromuscular Diseases, Uildm, Rome; †Division of Cardiology and ICU, St. Paolo Hospital Civitavecchia, Rome; ‡Division of Cardiology, San Filippo Neri Hospital, Rome; §Cardiovascular Diseases Department, Institute of Cardiology, Catholic University, Rome; ‖Division of Pediatric Cardiology, Bambino Gesù Hospital, Rome; ¶Muscular Dystrophy Research Unit, Institute of Neurology, Catholic University, Rome; and #Casa Sollievo della Sofferenza, San Giovanni Rotondo, Italy. This study was supported by Telethon Italy, grant 1153C.

Manuscript received November 8, 2002; revised manuscript received December 18, 2002, accepted January 24, 2003.

**Abbreviations and Acronyms**

cIBS = calibrated integrated backscatter
cvIBS = cyclic variation of integrated backscatter
DMD = Duchenne muscular dystrophy
DMDch = Duchenne muscular dystrophy children
ECG = electrocardiogram
EF = ejection fraction
IBS = integrated backscatter
ROI = region of interest
UTC = ultrasonic tissue characterization
Vcfc = rate-corrected velocity of circumferential fiber shortening

## METHODS

**Patients.** We enrolled 20 DMDch age 4 to 10 years (mean age 7 ± 2 years) followed at the Center for Neuromuscular Disease (Uildm of Rome, Italy) and 20 healthy, age-matched controls (mean age 8 ± 1 years, p = NS). None of the patients was under pharmacologic treatment. The study was approved by the Ethical Committee of Catholic University of Rome. Written informed consent was obtained in all cases.

In all patients, diagnosis of DMD was confirmed by muscle biopsy that showed the absence of dystrophin. In addition, an out-of-frame dystrophin gene deletion was found in 13 cases (Table 1). All DMDch had normal cardiologic examination, ECG, systolic function, and segmental wall motion at baseline echocardiography (Table 1). Ejection fraction (EF), calculated by Simpson's rule and Bullet methods, and rate-corrected velocity of circumferential fiber shortening (Vcfc) (10) were within normal limits in all patients. A detailed clinical and neurological examination was performed in all patients, including a standardized Gowers maneuver. For the purpose of this study, a significant muscle weakness was defined as the inability to stand up autonomously during the Gowers maneuver.

**Integrated backscatter (IBS) data acquisition and analysis.** We used a commercially available echocardiograph (Sonos 5500, Agilent, Andover, Massachusetts) equipped with a 2 to 4 MHz phased-array probe. Ultrasonic tissue characterization was performed by an Agilent Acoustic Densitometry software. The IBS data were displayed using a logarithmic scale in dB, with a dynamic processor range of 64 dB.

A preprocessing value of 1, a postprocessing gray-scale curve setting of A (the most linear setting), a transmit power of 35 dB, a mechanical index of 0.5, and a time-gain compensation of 140 dB were kept constant in all patients, all controls, and all horizontal image sections. This was easy to do because the population studied (children) was homogeneous for body habit. All images were obtained in the fundamental imaging mode. Acoustic densitometry image loops were acquired in digital format: 60 frames from consecutive cardiac cycles (2.48 s at 30 frames/s) were displayed after scan conversion and stored on optical disk for off-line analysis.

From the acoustic densitometry curve we measured two parameters: 1) the magnitude of cyclic variation of the IBS (cvIBS), which is the difference between the average peak (end-diastole) and average nadir (end-systole) values of IBS; and 2) the calibrated IBS (cIBS), which was derived from the absolute IBS value (Fig. 1). For IBS calibration we measured blood IBS with a circular-shaped region of interest (ROI) (41 × 41 pixels) in the left ventricular cavity at the mid-level (11).

All analyses were performed in the parasternal short-axis view (12). The UTC parameters such as cvIBS and cIBS have been shown (13,14) to depend significantly on the

**Table 1.** Clinical and Echocardiographic Data in Children With Duchenne Muscular Dystrophy

| Patient | Age (yrs) | Dystrophin Immunocytochemistry | Deletion | EF (%) | Vcfc (circ/s) | Muscle Weakness |
|---|---|---|---|---|---|---|
| 1 | 7.05 | Absent | Exons 5-7 | 61.2 | 1.33 | No |
| 2 | 4.05 | Absent | Exons 53-54 | 63.5 | 1.44 | No |
| 3 | 4.09 | Absent | Exon 52 | 67.1 | 1.32 | No |
| 4 | 7.06 | Absent | Exon 45 | 60.3 | 1.11 | No |
| 5 | 4.08 | Absent | ND | 63.9 | 0.949 | No |
| 6 | 4.06 | Absent | Exons 49-52 | 59.5 | 0.985 | No |
| 7 | 8 | Absent | Exon 45 | 59.6 | 0.853 | Yes |
| 8 | 4.03 | Absent | Exon 52 | 63.1 | 1.22 | No |
| 9 | 9 | Absent | Exons 45-50 | 56.4 | 0.702 | Yes |
| 10 | 6.02 | Absent | Exons 48-52 | 66.9 | 1.07 | No |
| 11 | 6.02 | Absent | ND | 61.7 | 1.07 | No |
| 12 | 7 | Absent | ND | 60.7 | 0.979 | No |
| 13 | 10 | Absent | ND | 63 | 1.28 | Yes |
| 14 | 8.03 | Absent | Exon 8 | 57.7 | 0.949 | No |
| 15 | 8.07 | Absent | ND | 55.9 | 1.1 | Yes |
| 16 | 10.02 | Absent | ND | 55.3 | 0.931 | No |
| 17 | 6.07 | Absent | ND | 56.5 | 0.906 | No |
| 18 | 8.08 | Absent | Exons 50-54 | 59.9 | 0.977 | No |
| 19 | 4.08 | Absent | Exons 45-52 | 62.8 | 1.66 | No |
| 20 | 8.04 | Absent | Exons 5-7 | 58.1 | 1.18 | Yes |

EF = ejection fraction; ND = not deleted; Vcfc = rate-corrected velocity of circumferential fiber shortening.

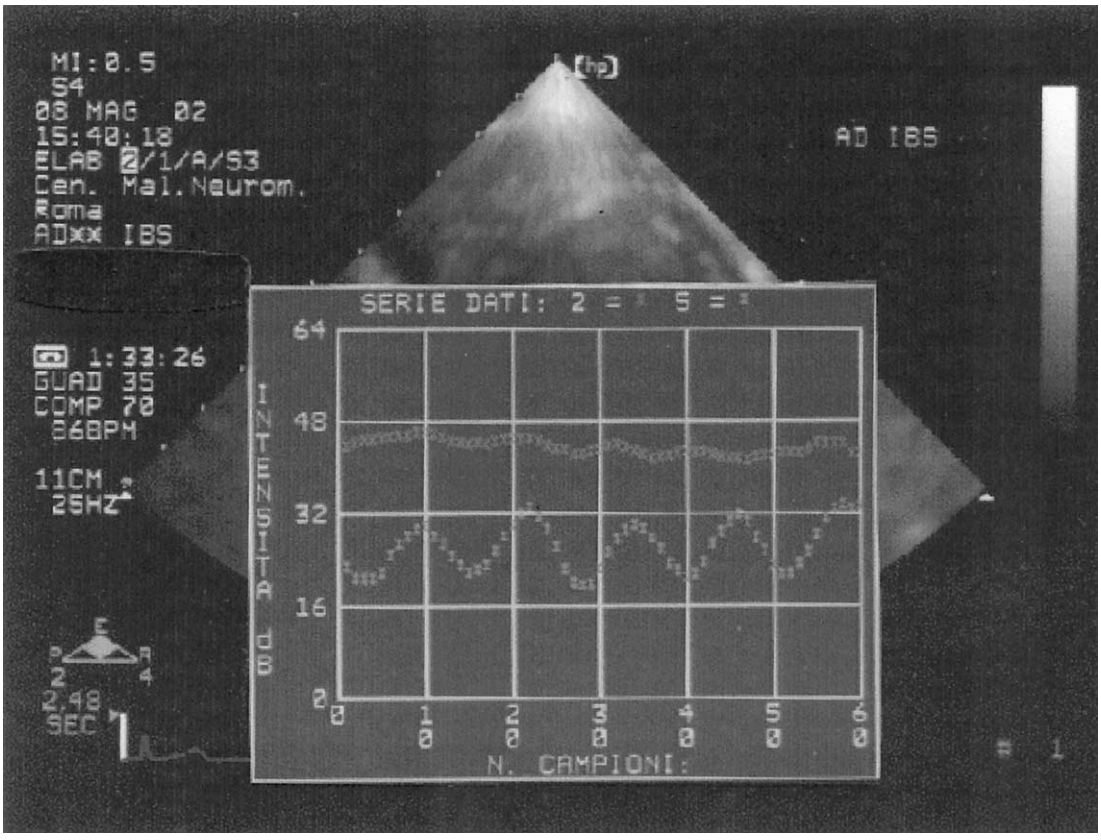


**Figure 1.** Plot of the cyclic variation of integrated backscatter (cvIBS) sampled on the inferior base segment and the calibrated integrated backscatter (cIBS) in a four-year-old Duchenne muscular dystrophy (DMD) child **(upper curve)** and in an age-matched control **(lower curve)**. The cvIBS and cIBS values are respectively smaller and higher in the DMD child than in the control.

angle between the ultrasonic beam and the myofiber direction, an effect known as anisotropy. To minimize the impact of myocardial anisotropy, we chose to analyze data from segments of the parasternal short-axis view in which the beam is approximately perpendicular to the local myofiber direction (Fig. 2). Locations at 5, 6, and 7 o'clock (corresponding to plb, ib, ilm, im, and ia; Fig. 2), satisfy this condition. Locations near 4 o'clock (alb, alm, and la; see Fig. 2) are somewhat less perpendicular.

The UTC parameters were measured at the basal, mid (papillary muscles), and apical levels during end-expiration. Circular, elliptical, and rectangular-shaped ROI (21 × 21 pixels) were placed in the midmyocardial layer of eight different myocardial segments (15) (Fig. 2). For both cvIBS and cIBS, the mean value obtained from the three ROIs was used for statistical analysis. To minimize high-frequency scatter noise we set the smoothing filters to a high level; lateral-gain compensation was not used in this study.

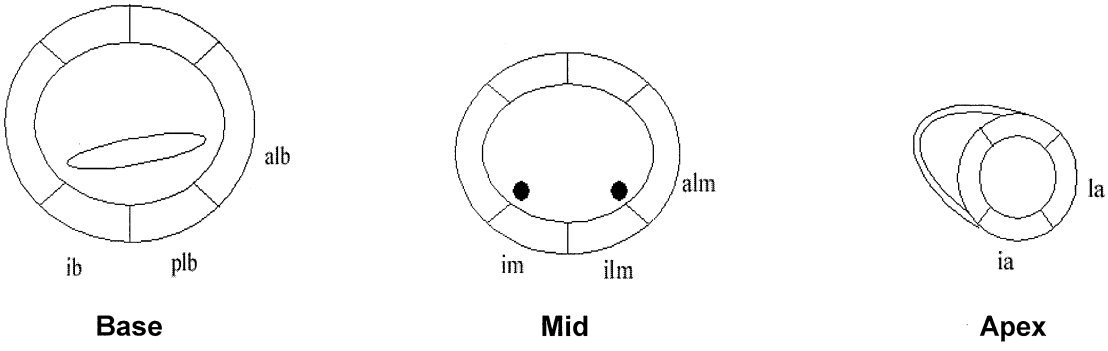


**Figure 2.** A 16-segment model was used for ultrasound tissue characterization analysis. The myocardial segments sampled were as follows: alb = anterolateral base; alm = anterolateral mid; ia = inferior apex; ib = inferior base; ilm = inferolateral mid; im = inferior mid; la = lateral apex; plb = posterolateral base.

**Table 2.** cIBS, cvIBS, and Time-Delay Mean Values in Children With Duchenne Muscular Dystrophy and Controls

| | Myocardial Segments (As Shown in Fig. 2) | | | | | | | |
|---|---|---|---|---|---|---|---|---|
| | **ib** | **plb** | **alb** | **im** | **ilm** | **alm** | **ia** | **la** |
| cIBS | | | | | | | | |
| DMDch | | | | | | | | |
| Mean | 37.0 | 41.0 | 33.6 | 35.7 | 41.3 | 31.9 | 37.3 | 32.7 |
| SD | 6.5 | 6.1 | 5.2 | 6.4 | 8.2 | 6.1 | 6.8 | 5.5 |
| Range | 21.7–41.7 | 27.7–51.1 | 24.2–40.1 | 23.4–46.1 | 26.7–57.9 | 22.2–42.4 | 24.9–45.0 | 24.0–40.6 |
| p | $<10^{-6}$ | $<10^{-6}$ | <0.0001 | <0.0003 | $<10^{-6}$ | <0.003 | <0.0001 | <0.0003 |
| Controls | | | | | | | | |
| Mean | 26.6 | 28.1 | 27.4 | 28.5 | 26.6 | 26.9 | 25.8 | 25.5 |
| SD | 1.5 | 2.3 | 1.5 | 1.8 | 2.1 | 1.6 | 1.7 | 1.6 |
| Range | 23.8–29.3 | 24.7–31.6 | 24.5–29.5 | 24.2–30.8 | 22.2–30.6 | 22.9–30.0 | 23.2–30.4 | 23.2–29.5 |
| cvIBS | | | | | | | | |
| DMDch | | | | | | | | |
| Mean | 4.1 | 4.2 | 4.4 | 4.7 | 4.5 | 4.0 | 5.6 | 4.0 |
| SD | 1.2 | 1.5 | 1.5 | 1.6 | 1.0 | 1.8 | 1.8 | 1.6 |
| Range | 2.4–6.6 | 2.1–8.3 | 2.2–9.2 | 2.5–9.6 | 2.5–6.7 | 2.0–9.2 | 3.4–9.5 | 2.0–7.2 |
| p | $<10^{-6}$ | $<10^{-6}$ | $<10^{-6}$ | $<10^{-6}$ | $<10^{-6}$ | $<10^{-6}$ | $<10^{-4}$ | $<10^{-6}$ |
| Controls | | | | | | | | |
| Mean | 8.6 | 8.7 | 8.4 | 9.4 | 8.8 | 9.0 | 8.7 | 8.7 |
| SD | 0.6 | 0.8 | 0.5 | 0.8 | 0.9 | 0.7 | 0.9 | 0.6 |
| Range | 7.7–10.0 | 7.3–10.5 | 7.6–9.4 | 7.8–10.8 | 7.4–11.4 | 7.0–10.0 | 7.3–10.1 | 7.6–9.5 |
| Time delay | | | | | | | | |
| DMDch | | | | | | | | |
| Mean | 1.5 | 1.2 | 2.6 | 1.6 | 1.2 | 2.5 | 1.6 | 2.6 |
| SD | 0.1 | 0.1 | 0.1 | 0.2 | 0.1 | 0.1 | 0.1 | 0.2 |
| p | NS | NS | NS | NS | NS | NS | NS | NS |
| Controls | | | | | | | | |
| Mean | 1.6 | 1.1 | 2.6 | 1.6 | 1.2 | 2.5 | 1.6 | 2.5 |
| SD | 0.1 | 0.1 | 0.1 | 0.2 | 0.1 | 0.1 | 0.1 | 0.2 |

Abbreviations as in Figure 1.

The time-delay value was calculated for each myocardial segment, in both patients and controls, as described elsewhere (16,17). Off-line analysis of cvIBS and cIBS data was performed by two blinded independent operators.

Interobserver reliability was tested on a sample of 40 myocardial segments. To test intraobserver reliability, the same 40 segments were re-evaluated after a 20-day period by one of the two observers. A good reproducibility of sampled data (<3% changes for each value) was obtained in both cases.

**Statistical analysis.** Intra- and interobserver variability of cvIBS and cIBS measurements were estimated by mean absolute differences between observations. Continuous variables between groups (patients and controls) were compared by *t* test for normally distributed values, as assessed by the Kolmogorov-Smirnov test (age, EF, etc.). All UTC parameters were compared using non-parametric statistics and the Mann-Whitney *U* test. The Bonferroni correction was applied when making multiple comparisons of the same variable (i.e., the comparison of UTC parameters in multiple myocardial segments, as shown in Table 2). Correlations were assessed by Spearman's rank correlation test. A value of $p < 0.05$ was considered significant. All values are shown as mean ± SD.

## RESULTS

**Echocardiographic data.** No significant differences were found in the mean values of EF and Vcfc between the DMDch and healthy controls (p = NS). The individual data from all patients are reported in Table 1.

**UTC analysis.** Analysis of both cvIBS and cIBS was performed on 160 segments in the controls (we studied 8 myocardial segments in each of 20 individuals). Only 145 segments were sampled in the DMDch, as the quality of imaging was inadequate for UTC analysis from both of the apical segments of the myocardium in six patients and from the 3 mid-segments in one patient. The DMDch and controls displayed different curves of data distribution for both cvIBS and cIBS (Fig. 3) ($p < 0.0001$ for both).

The mean value of cvIBS was 4.4 ± 1.5 dB (median 4.1 dB, range 2.0 to 9.6 dB) in DMDch and 8.8 ± 0.8 dB (median 8.8 dB, range 7.0 to 11.4 dB) in controls ($p < 0.0001$). The mean value of cIBS was 36.4 ± 7.1 dB (median 36.9 dB, range 21.7 to 57.9 dB) in DMDch, and 26.9 ± 2.0 dB (median 26.7 dB, range 22.2 to 31.6 dB) in controls ($p < 0.0001$).

In DMDch, the UTC changes occurred in all myocardial segments: each of the eight sampled segments displayed cIBS mean values significantly higher and cvIBS mean

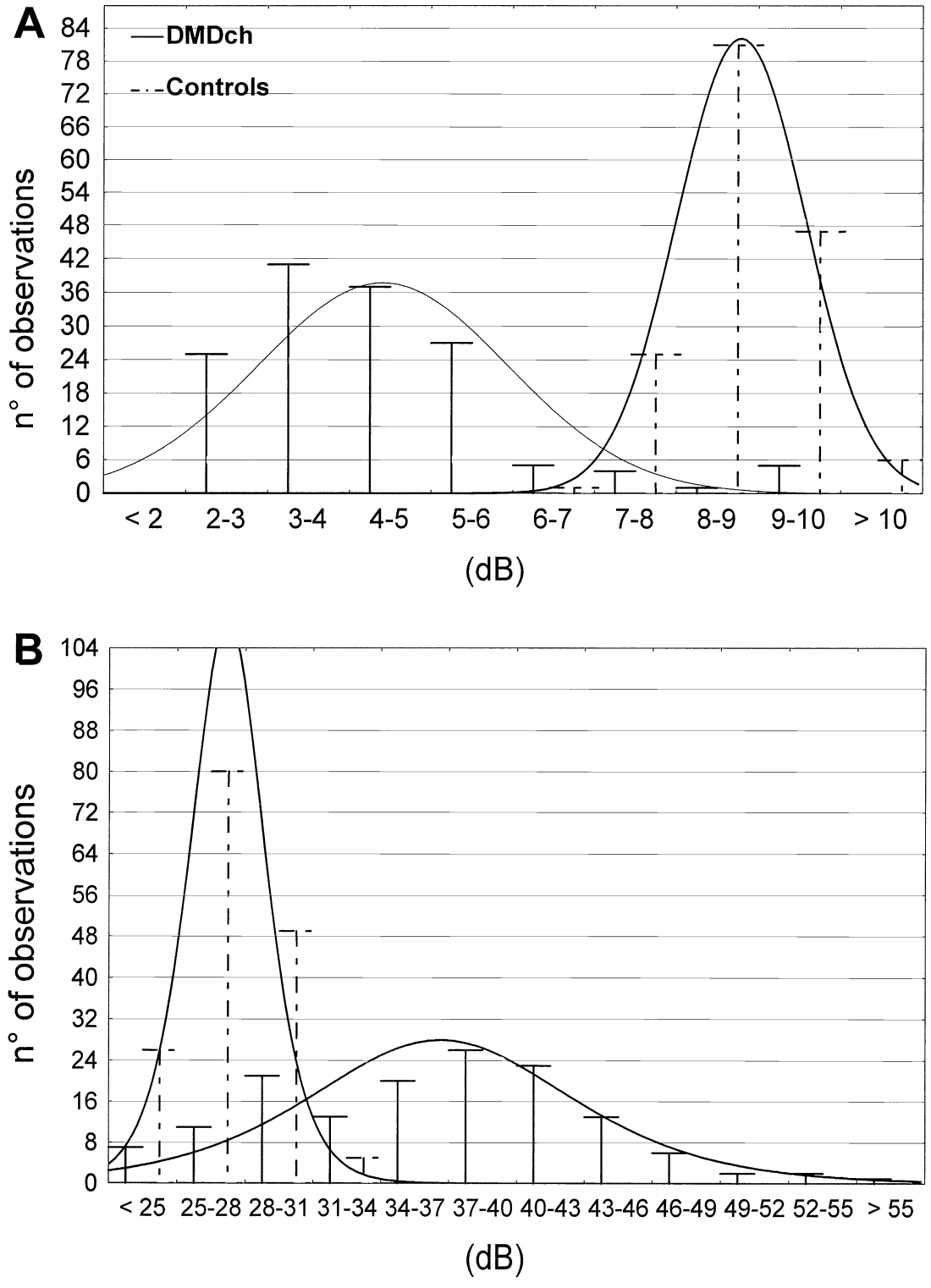


**Figure 3.** **(A)** Cyclic variation of integrated backscatter (cvIBS): data distribution in Duchenne muscular dystrophy children (DMDch) and controls. **(B)** Calibrated integrated backscatter (cIBS): data distribution in DMDch and controls.

values significantly lower than those of the same segments in age-matched healthy controls (see Table 2; all p values were calculated with Bonferroni correction, with n = 8 hypothesis tests). The standard deviation in both cvIBS and cIBS was also significantly higher in patients than in controls, indicating great variability in these parameters.

The mean value of the normalized time delay was similar in DMDch and controls in all myocardial segments

(Table 2). Time delays for those segments for which the ultrasonic beam is somewhat less perpendicular (segments alb, alm, and la) were longer than the time delays for segments near the 6 o'clock position (ib, plb, im, and ia; Fig. 2). Similarly, values of cIBS tended to be higher in the latter segments (Table 2). The cIBS values were only weakly correlated with cvIBS values, confirming that the two parameters reflect different acoustic properties of the myocardium.

**Single DMD patient study.** In controls, the mean value of cvIBS ranged between 8.1 and 9.6 dB, whereas 18 DMDch (90%) showed mean cvIBS values ranging between 3.4 and 5.3 dB; that is, <50% of the values of the control group. Only the remaining two patients showed different values: Patient #7 showed intermediate values that were between DMDch and controls (6.3 dB), and Patient #20 showed values near normal limits (with a mean 8.0 dB).

The mean values of cIBS in all sampled segments ranged between 25.4 and 27.9 dB in controls. In DMDch, cIBS mean values displayed a larger interval, ranging between 25.2 and 45.6 dB. It is worth noting that in only two patients the cIBS mean value fell within normal limits, and only one patient (Patient #20) had normal average values of both cIBS and cvIBS (but with a low value of cvIBS in three myocardial segments).

In patients there was no correlation between age and cIBS ($r = 0.22$; $p = 0.34$). However, there was a trend toward a positive correlation between age and cvIBS ($r = 0.40$; $p = 0.08$). These data indicate that the myocardial differences in UTC parameters between DMDch and controls do not increase with age but, for the cvIBS, they appear to be even more evident in younger children. There was no relationship between UTC parameters and muscle weakness assessed as ability to stand up autonomously.

## DISCUSSION

**Myocardial UTC properties.** Our results showed that UTC properties of the myocardium were clearly different in DMDch and in controls: in all sampled myocardial segments, cvIBS mean values were significantly lower and cIBS mean values significantly higher in DMDch than in age-matched healthy controls. In addition, for both parameters, DMDch displayed significant interindividual differences that were larger than those observed in controls. These findings show that early changes in myocardial features are common in young children with DMD, independent of the presence of ECG or two-dimensional echocardiographic anomalies.

The mechanisms underlying early UTC changes in DMDch are not completely clear. Both an increase in cIBS and a decrease in cvIBS have been correlated with collagen content and the development of fibrosis in human hearts and in experimental animals (18–24). It is possible that the UTC changes observed in DMDch may be secondary to significant myocardial fibrosis (which has been described in DMD patients with overt cardiomyopathy). Variations in the amplitude of cvIBS may also be caused by subtle changes in myocardial histological properties, reflecting water content, myofiber orientation, and size (25–28). Significant myocardial fibrosis is unlikely to be present in young DMDch with normal ECG and two-dimensional echocardiogram. This is supported by the lack of correlation between UTC changes and age (myocardial fibrosis is more likely to be present in older DMDch) and by the lack of perfusion/metabolism defects, as detected by positron emission tomography in DMDch younger than 11 years (29). In skeletal muscle, extensive fibrosis is prevalent in the latest stages of DMD, but more subtle changes can be present earlier and histological abnormalities are evident even during fetal life (3,4). Finally, the persistence of proteins expressed during fetal life has been suggested in DMDch by expression-profiling studies and confirmed by immunocytochemistry (30). Therefore, numerous histologic and structural modifications can be detected in the skeletal muscle of DMDch before muscle weakness and extensive fibrous tissue replacement begin; it is likely that similar modifications occur also in the myocardium.

In agreement with this hypothesis, cvIBS values similar to those we found in DMDch, i.e., a reduction of cvIBS values, have been described in normal myocardium during fetal life (31) and in the newborn. After birth, the level of cvIBS increases to that of infants and children in a few days or weeks (31). It is possible that the cardiomyocytes of DMDch retain features typical of fetal myocardial cells (in particular, the persistence of fetal proteins [30] or an increased water content). However, a specific assessment of the mechanisms of early UTC changes in DMDch would require a myocardial biopsy, which would seem unethical in this group of asymptomatic subjects.

The angle between the ultrasonic beam and the myofiber orientation may have important effects on UTC data (13,14). Indeed, in the present study, the values of time delays tended to be lower and cIBS higher in segments in which the beam was more perpendicular to the myofiber direction. However, this phenomenon cannot influence the results of our study because wide differences between patients and controls were observed in all myocardial segments studied.

Under some circumstances, the signals measured in the blood pool are dominated by clutter rather than by scattering from blood cells. Although we cannot rule out the possibility that the contributions of such clutter signals may degrade the accuracy of this approach obtaining an absolute calibration, the differences in cIBS data between DMDch patients and control subjects (Table 2) are so large that errors due to clutter appear not to be a factor in this study.

**Interindividual differences.** We are not surprised at the wide interindividual differences we found in the myocardium of DMDch (as opposed to the narrow range of UTC parameters in the controls) because the absence of dystrophin may cause tissue changes that can be represented in

different proportions in each patient and in different myocardial regions. However, despite this large interindividual variability, almost all DMDch showed large, significant UTC changes as compared with controls. These results strongly suggest that UTC changes are associated with an intrinsic, genetic change in myocardial features. No DMDch had normal UTC parameters values in all myocardial segments; only one DMDch (Patient #20, age 8.4 years) showed all cIBS values and 5 of 8 cvIBS values that were in the range of those in the control group. It is interesting to note that this child had clinical, biochemical, and molecular characteristics that did not differ from all other DMDch (in particular, there was evidence of dystrophin gene deletion and of significant muscle weakness). Patient #1, who carried the same deletion-encompassing exons 5 to 7 of the dystrophin gene, showed the highest cIBS mean value (i.e., the largest difference from controls in UTC) in the eight myocardial segments (average 45.6 dB) but had only minor muscle weakness.

Further studies in a wide group of patients and with a long-term follow-up would be required to assess whether the interindividual variation that we found in UTC may predict the onset of overt cardiomyopathy.

## CONCLUSIONS

Our results clearly show that subtle involvement of the myocardium is common in DMDch, and early changes in myocardial physical properties may easily occur independently from ECG or two-dimensional echocardiographic anomalies. Interindividual differences are also common among DMDch.

Because the identification of molecular markers associated with the progression of the disease in skeletal muscle promises to open the way to early genetic therapeutic treatment in DMD (32), the UTC technique may be a reliable tool for assessing myocardial changes as well as the effects of drugs (33) in longitudinal studies.

**Reprint requests and correspondence:** Dr. Vincenzo Giglio, Center for Neuromuscular Diseases, Uildm, Prospero Santacroce Street, 5, 00167 Rome, Italy. E-mail: giglio.echo@libero.it.

## REFERENCES

1. Rybakova IN, Patel JR, Davies KE, et al. The dystrophin complex forms a mechanically strong link between the sarcolemma and costameric actin. J Cell Biol 2000;150:1209–14.
2. Grady RM, Grange RW, Lau KS, et al. Role for alpha-dystrobrevin in the pathogenesis of dystrophin-dependent muscular dystrophies. Nat Cell Biol 1999;1:215–20.
3. Hudgson P, Pearse WG, Walton JN. Preclinical muscular dystrophy: histopathological changes observed in muscle biopsy. Brain 1967;90:565–6.
4. Mahoney MJ, Haseltine FT, Hobbins JC, et al. Prenatal diagnosis of Duchenne's muscular dystrophy. N Engl J Med 1977;297:968–73.
5. Muntoni F, Wilson L, Marrosu G, et al. A mutation in the dystrophin gene selectively affecting dystrophin expression in the heart. J Clin Invest 1996;96:693–9.
6. Frankel KA, Rosser RJ. The pathology of the heart in progressive muscular dystrophy: epimyocardial fibrosis. Hum Pathol 1976;7:375–86.
7. Sanjal SK, Johnson WW, Thapar MK, et al. An ultrastructural basis for electrocardiographic alterations associated with Duchenne's progressive muscular dystrophy. Circulation 1978;57:1122–9.
8. Nigro G, Politano L, Nigro V, et al. Mutation of dystrophin gene and cardiomyopathy. Neuromusc Disord 1994;4:371–9.
9. Mori K, Manabe T, Nii M, et al. Myocardial integrated ultrasound backscatter in patients with Duchenne's progressive muscular dystrophy. Heart 2001;86:341–2.
10. Colan SD, Borow KM, Neumann A. Left ventricular end-systolic wall stress-velocity of fiber shortening relation: a load-independent index of myocardial contractility. J Am Coll Cardiol 1984;4:715–24.
11. Naito J, Masuyama T, Mano T, et al. Validation of transthoracic myocardial ultrasonic tissue characterization: comparison of transthoracic and open-chest measurements of integrated backscatter. Ultrasound Med Biol 1995;21:33–49.
12. Stuhlmuller JE, Skorton DJ, Burns TL, et al. Reproducibility of quantitative backscatter echocardiographic imaging in normal subjects. Am J Cardiol 1992;69:542–6.
13. Recchia D, Miller JG, Wickline A. Quantification of ultrasonic anisotropy in normal myocardium with lateral gain compensation of two-dimensional integrated backscatter images. Ultrasound Med Biol 1993;19:497–505.
14. Holland MR, Wilkenshoff UM, Finch-Johnston AE, et al. Effects of myocardial fiber orientation in echocardiography: quantitative measurements and computer simulation of the regional dependence of backscattered ultrasound in the parasternal short-axis view. J Am Soc Echocardiogr 1998;11:929–37.
15. Shiller N, Shah PM, Crawford M, et al. Recommendations for quantitation of the left ventricle by two-dimensional echocardiography. J Am Soc Echocardiogr 1989;2:358–67.
16. Mohr GA, Vered Z, Barzilai B, et al. Automated determination of the magnitude and time delay ("phase") of the cardiac cycle dependent variation of myocardial ultrasonic integrated backscatter. Ultrasound Imaging 1989;11:245–9.
17. Finch-Johnston AE, Gussak HM, Mobley J, et al. Cyclic variation of integrated backscatter: dependence of time delay on the echocardiographic views used and the myocardial segment analized. J Am Soc Echocardiogr 2000;3:9–17.
18. Perez JE, Barzilai B, Madaras EI, et al. Applicability of ultrasonic tissue characterization for longitudinal assessment and differentiation of calcification and fibrosis in cardiomyophathy. J Am Coll Cardiol 1984;4:88–95.
19. Hoyt RH, Collins SM, Skorton DJ, et al. Assessment of fibrosis in infarcted human hearts by analysis of ultrasonic backscatter. Circulation 1985;71:740–4.
20. Hoyt RH, Skorton DJ, Collins SM, et al. Ultrasonic backscatter and collagen in normal ventricular myocardium. Circulation 1984;69:775–82.
21. Naito J, Masuyama T, Mano T, et al. Ultrasonic myocardial tissue characterization in patients with dilated cardiomyopathy: value in noninvasive assessment of myocardial fibrosis. Am Heart J 1996;131:115–21.
22. Masuyama T, Nellessen U, Schnittger I, et al. Ultrasonic tissue characterization with a real-time integrated backscatter imaging system in normal and aging human hearts. J Am Coll Cardiol 1989;14:1702–8.
23. Vered Z, Barzilai B, Mohr GA, et al. Quantitative ultrasonic tissue characterization with real-time integrated backscatter imaging in normal human subjects and in patients with dilated cardiomyopathy. Circulation 1987;76:1067–73.
24. Milunski MR, Mohr GA, Perez JE, et al. Ultrasonic tissue characterization with integrated backscatter: acute myocardial ischemia, reperfusion and stunned myocardium in patients. Circulation 1989;80:491–503.
25. O'Brien PD, O'Brien WD, Rhyne TL, et al. Relation of ultrasonic backscatter and acoustic propagation properties to myofibrillar lenght and myocardial thickness. Circulation 1995;91:171–5.
26. Sagar KB, Pelc LE, Rhyne TL, et al. Influence of heart rate, preload, afterload, and inotropic state on myocardial ultrasonic backscatter. Circulation 1988;83:762–9.

27. Wickline SA, Thomas LJ, Miller JG, et al. The dependence of myocardial ultrasonic integrated backscatter on contractile performance. Circulation 1985;72:183–92.
28. Wickline SA, Thomas LJ, Miller JG, et al. A relationship between ultrasonic integrated backscatter and myocardial contractile function. J Clin Invest 1985;76:2151–60.
29. Quinlivan RM, Lewis P, Marsden P, et al. Cardiac function metabolism and perfusion in Duchenne and Becker muscular dystrophy. Neuromusc Disord 1996;6:237–46.
30. Chen YW, Zhao P, Borup R, et al. Expression profiling in the muscular dystrophies: identification of novel aspects of molecular pathophysiology. J Cell Biol 2000;151:1321–36.
31. Goens MB, Karr SS, Martin GR. Cyclic variation of integrated ultrasound backscatter: normal and abnormal myocardial patterns in children. J Am Soc Echocardiogr 1996;9:616–21.
32. Chamberlain JS. Muscular dystrophy meets the gene chip: new insights into disease pathogenesis. J Cell Biol 2000;151:F43–6.
33. Suwa M, Ito T, Kobashi A, et al. Myocardial integrated ultrasonic backscatter in patients with dilated cardiomyopathy: prediction of response to beta-blocker therapy. Am Heart J 2000;139:905–12.